1

Semiconductor Lasers and VCSEL History

Kenichi Iga

1.1 History and Basics of Semiconductor Lasers

The vertical-cavity surface-emitting laser (VCSEL, pronounced "vic-cell") is a special class of semiconductor laser that emits coherent, or laser, light orthogonally to the semiconductor substrate as shown in the schematic in Figure 1.1. The VCSEL device and its applications are the core subject of this book. This VCSEL structure generates a host of industrial applications that will be introduced comprehensively throughout this book. Before starting with a history of VCSELs, let us begin with some basic concepts of semiconductor lasers to aid in the understanding of the following chapters for general readers.

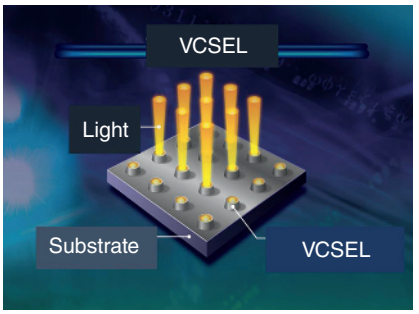

Figure 1.1 Schematic of a vertical-cavity surface-emitting laser (VCSEL). *Source:* Figure by K. Iga [copyright reserved by author].

1.1.1 Categorization of Semiconductor Lasers

Semiconductor lasers can be categorized into several types depending on:

i) Emission wavelength and materials;
ii) Resonant cavity configuration;
iii) Single mode or multi-mode;
iv) Direction of emitted light;
v) Direct modulation speed;
vi) Power output;
vii) Footprint of device;
viii) Beam form and connectivity to optics such as optical fibers;

VCSEL Industry: Communication and Sensing, First Edition. Babu Dayal Padullaparthi, Jim A. Tatum and Kenichi Iga.

ix) Price of device;
x) Manufacture volume;
xi) 1D or 2D array; and so on.

A simple category is outlined in Table 1.1. In this case, we categorized into two types on the basis of cavity configuration, i.e., edge- and surface-emitting cavities. This book is focused on the research, development, and industrial sectors to demonstrate the impact of **VCSEL**.

A schematic of an edge-emitting laser (EEL) is shown in Figure 1.2a. In edge-emitting lasers, the light emits through the edges of the wafer that is in-plane with the substrate and the optical cavity is horizontal for laser resonance. On the other hand, the structure of VCSEL is illustrated in Figure 1.2b. The resonance of light is vertical to the substrate and taken from the surface. The laser structure is formed on the substrate in just one manufacturing process.

Table 1.1 Categorization of semiconductor lasers.

Type of cavity	Edge-emitting laser	Surface-emitting laser
Single Mode		
Transverse	narrow stripe	narrow aperture
Wavelength	DFB, DBR	Fabry-Pérot
Multi-Mode		
Transverse	broad area	wide aperture
Wavelength	Fabry-Pérot	Fabry-Pérot
Array	one-dimensional	two-dimensional

Source: Table by K. Iga [copyright reserved by author].

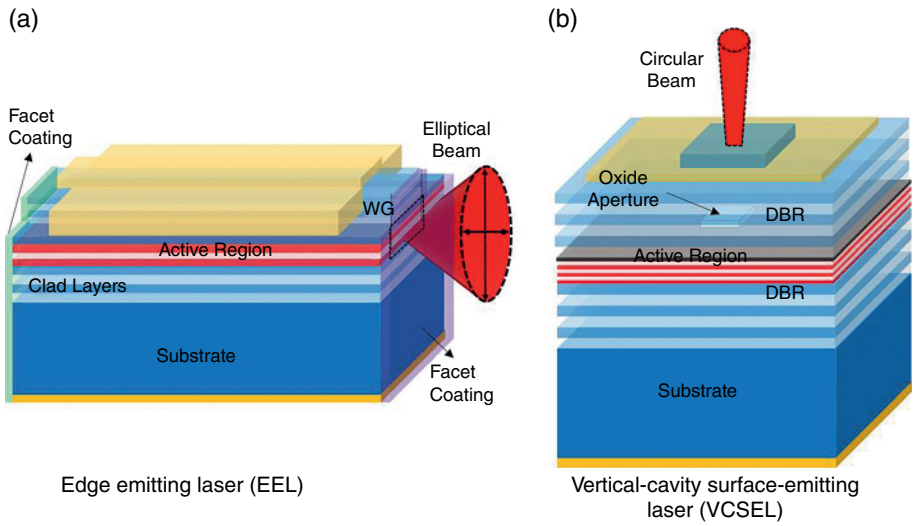

Figure 1.2 Schematic of semiconductor lasers (a) Edge-emitting laser (EEL). (b) Vertical-cavity surface-emitting laser (VCSEL). *Source:* Figure by B. D. Padullaparthi [copyright reserved by authors].

In both cases, the emission and amplification of light in semiconductor lasers is due to the recombination of electrons and holes that exist in the active region. This is what most of the standard textbooks on optical properties of semiconductors teach. Later, we will show the readers a different explanation.

1.1.2 Light Emission and Absorption in Semiconductors

The characteristics of the semiconductor diode current (*I*) as a function of the applied voltage (*V*) are used to create several different types of optical devices. The voltage–current (*V-I*) characteristic of a diode is shown in Figure 1.3. The first quadrant Q1 is known as forward bias, and the current increases exponentially with the applied voltage. When an electron and a hole recombine near the p-n junction, the energy is released as a photon. This regime is where light-emitting diodes (LEDs) and lasers operate.

The third quadrant Q3 is the reverse bias region, which is used as photodetectors. When a photon is absorbed near the p-n junction, the light energy creates an electron and hole pair. The electrons drift to the positive electrode and the holes move to the negative electrode under reverse bias.

The fourth quadrant Q4 is where photoconduction occurs and is the operating regime for solar cells. When a photon is absorbed near the p-n region, an electron hole pair is created. The resultant current times voltage (power) generates an electrical energy in the solar cell. The second quadrant is not used for practical optical devices.

The first and third quadrants play critical roles as key optoelectronics components for optical communication and sensing applications. To understand how light (photons) interacts with semiconductors, a deeper understanding of light emissions and absorption is needed.

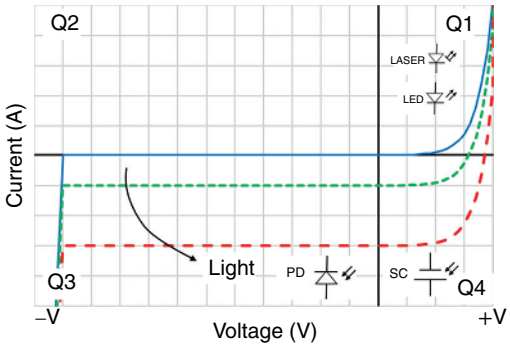

Figure 1.3 Voltage–current (V–I) characteristic of a p-n junction with no incident light (solid curve) and with incident light (dashed curves). *Source:* Figure by K. Iga and J. A. Tatum [copyright reserved by authors].

1.1.3 Birth of Semiconductor Lasers

1.1.3.1 Homostructure and Double Heterostructure Lasers

Based on the principle of light amplification in semiconductors, the first semiconductor laser was realized by four groups almost simultaneously in 1962. This was two years later after Therdore Maiman demonstrated the first laser [1]. The optical gain layer was located near the p-n homojunction parallel to the substrate [2–5]. The light resonance occurs between the mirrors formed at the edge of the substrate by cleaving or polishing the semiconductor crystal. These lasers are known as edge-emitting lasers (EELs).

In 1970, eight years later, two groups reported a double heterostructure (DH)-based laser that enabled room-temperature continuous operation [6, 7]. The device using an AlGaAs-GaAs DH

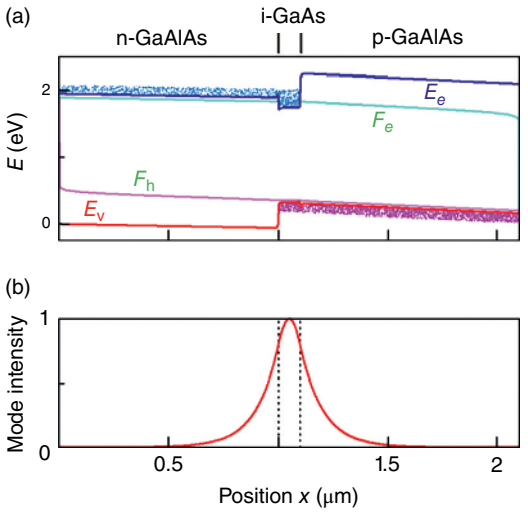

Figure 1.4 Double heterostructure laser. (a) The carrier densities of electron and holes in p, i, and n regions. (b) The optical field intensity near the double heterostructure. *Source:* [8]. [Image courtesy of Genichi Hatakoshi.]

structure, as shown in Figure 1.4, introduced by Hayashi and Panish reduced the threshold current density to about 1 kA/cm^2 at 300 K, a major breakthrough over the initial homo-junction devices.

Back in 1963, a double heterostructure laser had been proposed by Herbert Kromer by using semiconductor layers with varying bandgap and refractive index [9]. Herbert Kroemer and Zhores Alferov [7] both received the 2000 Nobel Prize in Physics for the idea.

This DH structure is used only for confining light field as shown in Figure 1.4b. More descriptions can be found in related textbooks [10–14].

1.1.3.2 Quantum Well Lasers

Present semiconductor lasers utilize quantum wells (QWs) as shown in Figure 1.5 for the light emitting and amplification layer for almost all semiconductor lasers and LEDs. The QW [15] has a thickness of several nanometers (1 nm = 10^{-9} m). Grain-shaped quantum dots [16, 17] that have a several-nanometer box size can be used to further reduce the threshold current in semiconductor lasers. The optical gain necessary for lasing using multiple quantum wells (MQWs) is further explained in Chapter 2.

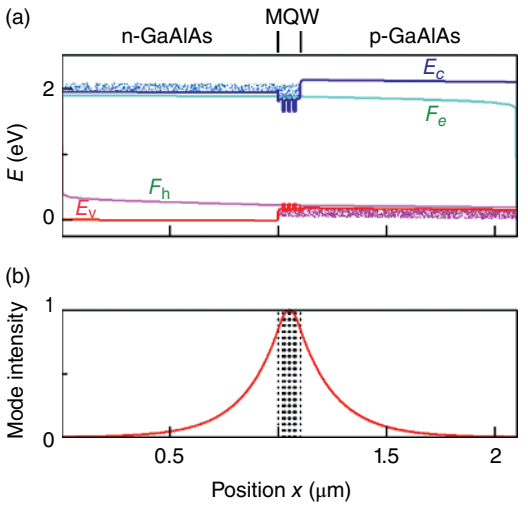

Figure 1.5 Quantum well structure with separate optical confinement. (a) The carrier densities of electron and holes in a quantum well structure. (b) The quantum well laser where the optical field is confined by the double heterostructure. *Source:* [8]. [Image Courtesy of Genichi Hatakoshi.]

1.1.4 Amplification of Light in Semiconductors

The relationship between the density of states and energy in semiconductors is shown in Figure 1.6. This is determined by the product of the parabolic density of states in the conduction band and the valence band and the Fermi-Dirac distribution according to Pauli exclusion principle. In the case of bulk semiconductors, it has the shape shown in the Figure 1.6. E_c and E_v are Fermi levels in thermal equilibrium in the conduction band and valence band, respectively, and E_g is the bandgap energy. If the electrons and holes are excessive due to photoexcitation or current injection, the distribution changes. The electron and hole levels in each band are called quasi- or degenerate-Fermi level and are indicated by E_{fc} and E_{fv}. The condition for the population inversion from the thermal equilibrium state (also called quasi equilibrium) is expressed by:

$E_{fc} - E_{fv} > E_c - E_v$: negative temperature or amplifying (condition for gain).

When the light with angular frequency ω comes in the semiconductor, the following characteristics appear, where $\hbar$ is the reduced Planck's constant: $\hbar = h/2\pi$ (h: Planck's constant). Here, $\hbar\omega$ is a quantized photon energy, which appears in Chapter 8.

$\hbar\omega < E_c - E_v$: transparent
$\hbar\omega > E_c - E_v$: absorptive

As shown in Figure 1.6, in the excited state, the carrier distribution representing the gain is distributed in a mountain shape with respect to energy. The result of the calculation is also shown in Figure 1.7.

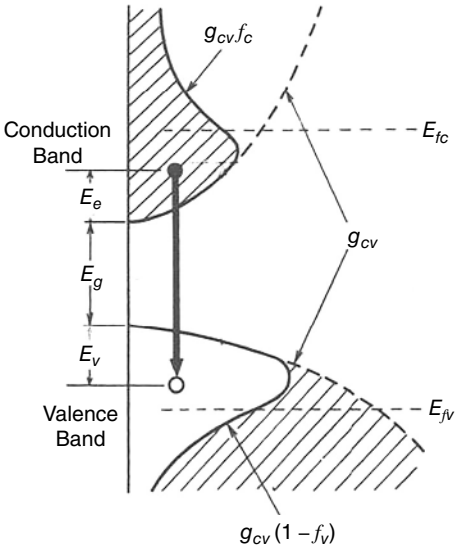

Figure 1.6 Population distribution of electrons and holes in semiconductor well vs. energy. *Source:* [18]. (After Masahiro Asada and Yasuharu Suematsu)

Figure 1.7 Optical gain of semiconductor vs. energy. *Source:* [19]. (After Masahiro Asada and Yasuharu Suematsu)

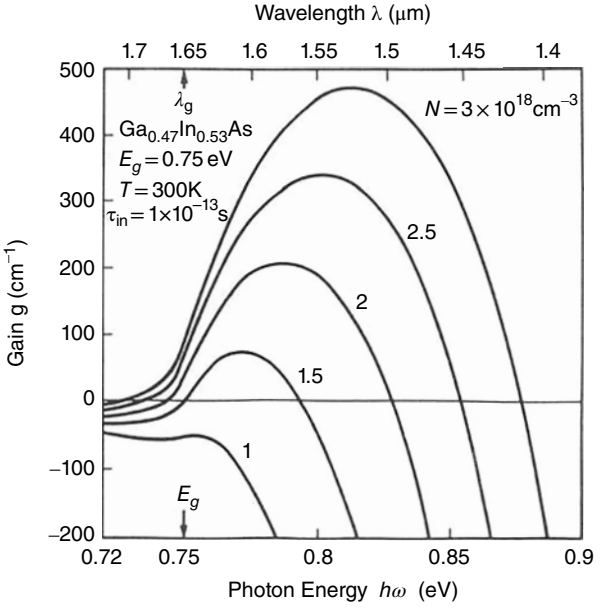

1.1.5 Oscillation Conditions in Semiconductor Lasers

1.1.5.1 Laser Resonators

The schematics of the edge- and surface-emitting laser (VCSEL) are shown in Figure 1.8. The edge-emitting (EE) laser, shown in Figure 1.8(a), includes Fabry-Pérot (FP) laser, distributed feedback (DFB) laser, and distributed Bragg reflector (DBR) laser. These laser types will be compared with VCSEL in Figure 1.8b in subsequent chapters.

Let us consider the oscillation conditions of a semiconductor laser. As shown in Figure 1.8(a) and (b), the target semiconductor laser is composed of a Fabry-Pérot (FP) cavity. Both resonators are generalized in Figure 1.9(a). By using the field reflectance including phase shift, which will be given later, this model can be applied to edge-emitting Fabry-Pérot lasers, DFB lasers, DBR lasers, and VCSELs as well.

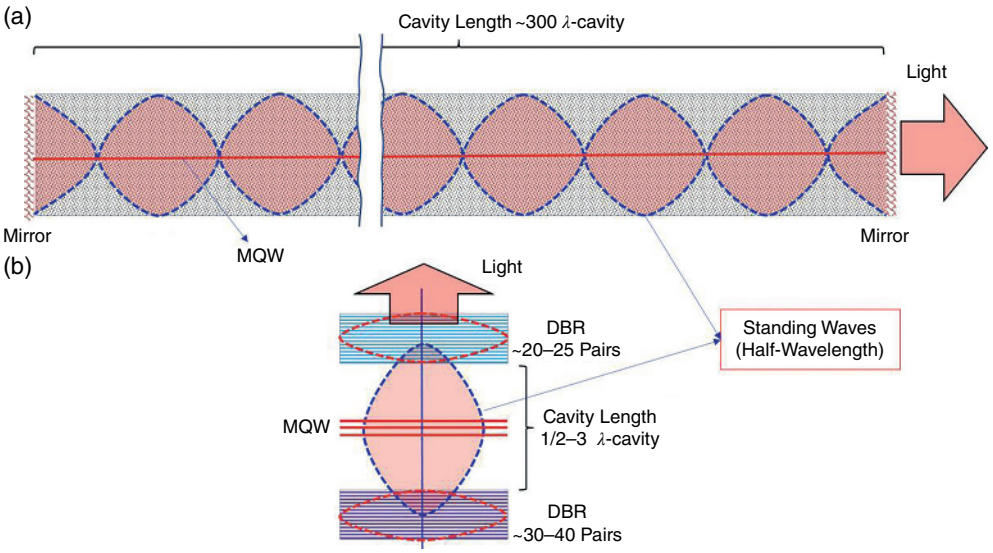

Figure 1.8 Schematic of edge-emitting Fabry-Pérot lasers and VCSELs. The coupling of light through standing waves in laser resonators (a) Fabry-Pérot (edge-emitting laser/EEL), and (b) surface emitting laser (VCSEL). *Source:* Figure by K. Iga and B. D. Padullaparthi [copyright reserved by authors].

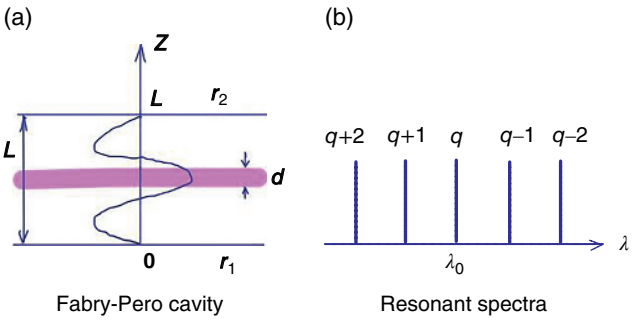

Figure 1.9 Fabry-Pérot cavity and resonant spectra. (a) Fabry-Pérot cavity. (b) Resonant spectra.

<Parameters>
L: cavity length
d: thickness of active layer
ϕ_1, ϕ_2: phase shift of each reflection
r_1, r_2: electric field reflectance coefficients of the mirrors at both ends
R_1, R_2,: power reflection coefficients of the mirrors at both ends

$$r_1 = \sqrt{R_1}\,\mathrm{e}^{-j\phi_1}$$

$$r_2 = \sqrt{R_2}\,\mathrm{e}^{-j\phi_2}$$

g: gain coefficient
α: loss coefficient
β: propagation constant ($=w/c = 2\pi f/c$)
ω: angular frequency

Consider that the light wave in the resonator travels in the z direction from $z = 0$ and is reflected by the reflector r_2 at $z = L$; then it goes backward by the length of L and returns to the starting point $z = 0$. If the electric field is sustainable, we should have:

$$\sqrt{R_1R_2}\,e^{-j\left(2\beta L+\phi_1+\phi_2\right)}e^{\left(gd-\alpha L\right)} = 1 \tag{1.1}$$

By comparing the imaginary and real parts, we have:

$$2\beta L + \phi_1 + \phi_2 = 2\pi q\left(q = \text{integer}\right)\left\langle\text{resonance conditions}\right\rangle \tag{1.2a}$$

$$\sqrt{R_1R_2}\,\exp\left[\left(gd-\alpha L\right)\right] = 1\left\langle\text{gain condition}\right\rangle. \tag{1.2b}$$

For the threshold gain g_{th} required for oscillation, use *ln*, the natural logarithm; from Eq. (1.2b),

$$g_{th} = \alpha\frac{L}{d} + \frac{1}{2d}\ln\left(\frac{1}{R_1R_2}\right). \tag{1.3}$$

The first term is absorption by the medium, and in GaAs, absorption by the free carrier has a magnitude of about 10 cm^{-1}. In the second term, the reflectance of a reflector made by cleaving the surface of a semiconductor is

$$R_1 = R_2 = R = \left\{\left(n-1\right)/\left(n+1\right)\right\}^2 \quad \left(n:\text{Equivalent refractive index of semiconductor}\right) \tag{1.4}$$

Therefore, in the case of a GaAs edge-emitting laser ($n = 3.5$) with $L = d = 300$ μm, it is about 39 cm^{-1}. To oscillate, a threshold gain of 10 + 39 = 49 cm^{-1} or more is required.

The electric field E_{out} of the output light, with E_0: field at the end of cavity, is given by:

$$E_{out} = \sqrt{1-R_2}\;E_0. \tag{1.5}$$

1.1.5.2 Resonant Wavelength

Now, if λ denotes the wavelength and n the equivalent refractive index, from Eq. (1.2a) we have:

$$2\left(2\pi n/\lambda\right)L + \phi_1\left(\lambda\right) + \phi_2\left(\lambda\right) = 2\pi\mathrm{q}\left(\mathrm{q}:\text{integer}\right). \tag{1.6}$$

When the phase shift is 0 and the reflector is at the fixed end, for example, the standing wave is as shown in Figure 1.8b. The total length L is an integer q times the half wavelength $\lambda/(2n)$ in the medium:

$$\left(\lambda/2n\right)q = L. \tag{1.7}$$

Now, in a laser cavity with a resonator length L longer than the wavelength, waves of many wavelengths with slightly different lengths can resonate. These modes are called longitudinal modes. On the other hand, the modes in the perpendicular direction are called the transverse modes.

Considering a normal semiconductor laser, if λ is 1.3 μm, $n = 3.5$, and $L = 3$ μm, then $q = 16$.

Therefore, even if q differs by 1, the resonance wavelength changes only slightly as $\Delta\lambda$. With $|\Delta\lambda| \ll \lambda$ in mind, if $\lambda \to \lambda_0 + \Delta\lambda$, $q \to q + 1$, then we obtain,

$$\frac{\Delta\lambda}{\lambda_0} = -2\frac{\lambda_0}{n_{eff}L}. \tag{1.8}$$

This $|\Delta\lambda|$ is called free spectral range (FSR) and is inversely proportional to cavity length, L.

Here, n_{eff} is the effective index considering the dispersion of the medium and is given by the following expression:

$$n_{eff} = n\left\{1 - \left(\lambda_0/n\right)\left(\partial n/\partial\lambda\right)\Big|_{\lambda=\lambda_0}\right\}. \tag{1.9}$$

Since $\partial n/\partial\lambda < 0$ in ordinary semiconductors, n_{eff} is usually larger than n. In the above example, $n_{\text{eff}} = 4.0$ and $|\Delta\lambda| = 70$ nm.

1.1.5.3 Cavity Formation

To achieve laser oscillation, a resonator that provides optical feedback to the gain medium is required. The laser resonator is formed by a pair of mirrors; a so-called Fabry-Pérot (FP) resonator is shown in Figure 1.8(a). In an edge-emitting laser, the gain width is *w,* the cavity length is equal to L, and the mirror is usually made by simply cleaving the semiconductor crystal. In this case the refractive index of about 3.5 is higher than outside air, and the resonator edges look like open termination. (Here $\phi = 2\pi$. ϕ is defined in Eq. (1.1)).

In Table 1.1 we have touched on DFB and DBR structures for single-mode operation of edge-emitting lasers [20–23]. In both cases, we utilize a pair of Bragg mirrors having an electric field reflectivity expressed by $r = \sqrt{R}\exp\left(-j\phi\right)$ that sandwich some space or active region. These wavelength-selective cavities can provide single longitudinal-mode operation. For using those lasers in optical pulse code modulation (PCM) for optical fiber communications, they should maintain single mode under high-speed modulation (~100 Gb/s). Moreover, in the case of coherent digital communications, the laser should operate with narrow spectrum (~kHz). This kind of lasers is called a dynamic single-mode laser [24].

In the case of VCSELs the mirrors are formed by semiconductor Bragg reflectors or dielectric mirrors, and therefore, we can design the resonator as open or short terminations. We can use its large free spectral range (FSR) for pure single longitudinal-mode operation and wide-range wavelength tuning. The details will be described in Chapters 2 and 8.

1.2 Semiconductor Lasers and Manufacturing

1.2.1 Manufacturing Process of Edge-Emitting Lasers

A schematic of EEL manufacturing and testing processes is shown in Figure 1.10. The edge-emitting lasers (such as FP and DFB lasers) require facet coatings after cleaving and often need regrowth of specific steps.

The FP-EELs with cleaved laser mirrors have only 33% reflectivity. The reflectivity of the cleaved surface can be modified to be either higher or lower reflectivity by coating multi-layer films that can be used to optimize the performance characteristics and to protect the surfaces of the EEL. The facet coatings are applied after the lasers are cleaved from the substrate and require extensive handling, which makes them more difficult to manufacture.

Another approach is to form the distributed reflectors through multiple epitaxial steps with intermediate fabrication steps. The regrowth and the intermediate processing result in a nonmonolithic epitaxial growth making this process very complex and not manufacturing-friendly compared to a fully monolithic VCSEL fabrication.

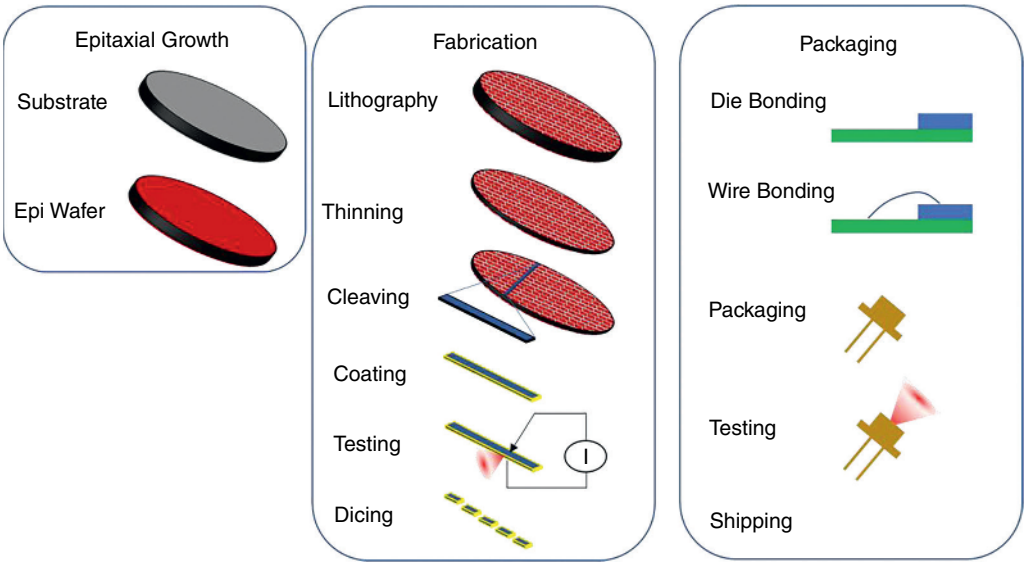

Figure 1.10 The manufacturing processes of edge-emitting lasers. *Source:* Figure by K. Iga and J. A. Tatum [copyright reserved by authors].

1.2.2 Vertical-Cavity Surface-Emitting Laser

In vertical-cavity surface-emitting lasers, the optical cavity is designed to be normal to the wafer surface, and the light emits vertically from the surface, as shown in Figure 1.2(b). High reflectivity mirrors (>99%) can be obtained with the growth of multiple epitaxial layers just above and below the active cavity without regrowth, resulting in an optical resonator cavity on the order of the emission wavelength, which is often referred to as a microcavity resonator. The lateral optical and electrical confinement is achieved by an oxidation process and may have sizes from one to several

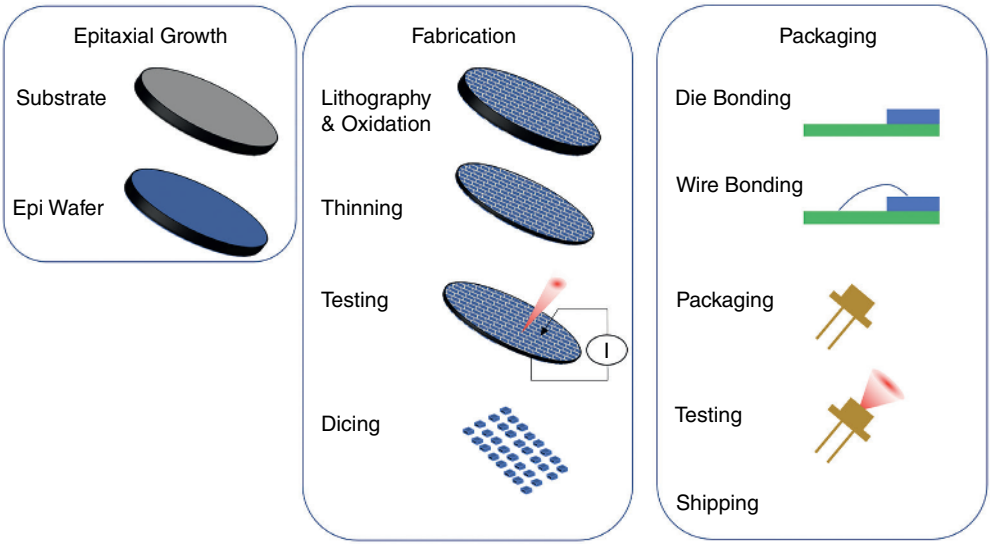

Figure 1.11 The manufacturing and testing processes of VCSELs. *Source:* Figure by K. Iga and J. A. Tatum [copyright reserved by authors].

tens of microns. This lateral size controls the mode profile of the laser and will be further described in Chapter 2.

As shown in Figure 1.11, the epi-growth process is fully monolithic and device fabrication is manufacturing-friendly and scalable. Mass production of VCSELs thus appears more like modern LED and IC manufacturing. In contrast to FP-edge-emitting lasers, the handling of full wafers only (no bar handling or facet coatings), the ability of fully testing on wafer (see Appendix D), and the knowledge of yield at that point result in a lower cost for VCSELs.

Since 2020, VCSELs are manufactured on wafer diameters of 150 mm diameters and as previously described are compatible with high-volume III–V semiconductor manufacturing processes. Many tens to hundreds of thousands of VCSELs can be fabricated on a single 150 mm wafer. With dramatic improvements in the epitaxial and fabrication processes, the device yields are routinely in excess of 90%. Details of wafer size and die counts will be given in Chapter 3. An example of fully processed VCSEL epitaxial wafer (so-called deliverable-wafer) is shown in Figure 1.12.

Figure 1.12 A fully processed VCSEL layer structure on 6″ (150 mm) GaAs substrate. *Source:* Wafer photo by Jim A. Tatum, Dallas, Texas, USA. [copyright reserved].

1.3 VCSEL History and Development

During the four decades since the initial VCSEL conception in 1977, many hundreds of millions of VCSELs have been shipped from a large number of VCSEL manufacturers. Some of the more ubiquitous examples are laser printers, bar code scanners, computer mice, high-speed data communications over fiber optic networks, 3D sensing in consumer and automotive electronics, night vision equipment, and many more industrial and consumer devices. It is not surprising to say that VCSELs have affected the life of nearly every person and household. With this background, we present a brief history of VCSELs from its birth to today's use in many commercial products. We divide the time in five different periods to describe the generations of VCSEL development as shown in Figure 1.13 and detail the stages in the following paragraphs.

1.3.1 Stage I: Initial Concept and Invention

1.3.1.1 Stage Ia: Invention and Initial Demonstration

Now, what is this new surface-emitting laser (SEL) or the vertical-cavity surface-emitting laser (VCSEL)? The structure is substantially different from conventional edge-emitting lasers (EELs), i.e., the vertical cavity is formed by the surfaces of epitaxial layers, and light output is from one of the mirror surfaces orthogonal to the substrate as has been shown in Figure 1.13. It is recognized that one of the authors (Iga, from Tokyo Institute of Technology) invented VCSEL in 1977 [25–28] as shown in the inset of Figure 1.13. This new invention was coined VCSEL (vertical-cavity surface-emitting laser), following the naming of a "pixel," which means any of the small discrete elements that together constitute an image (as on a television or digital

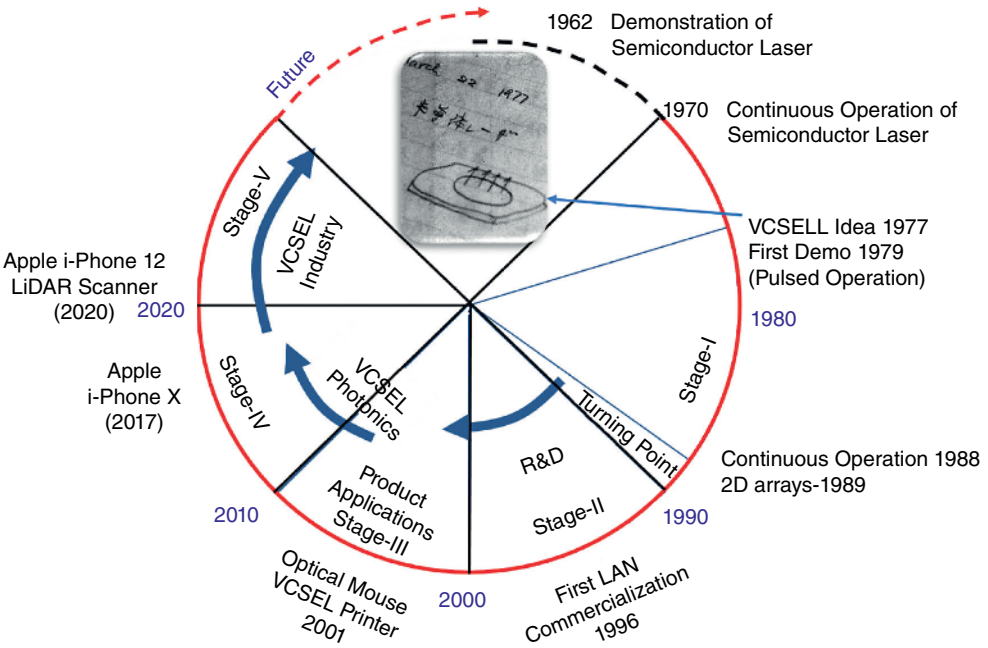

Figure 1.13 Stages of VCSEL development. The inset figure shows the sketch of VCSEL drawn by Kenichi Iga on March 22, 1977. *Source:* Figure by K. Iga and B. D. Padullaparthi [copyright reserved by authors].

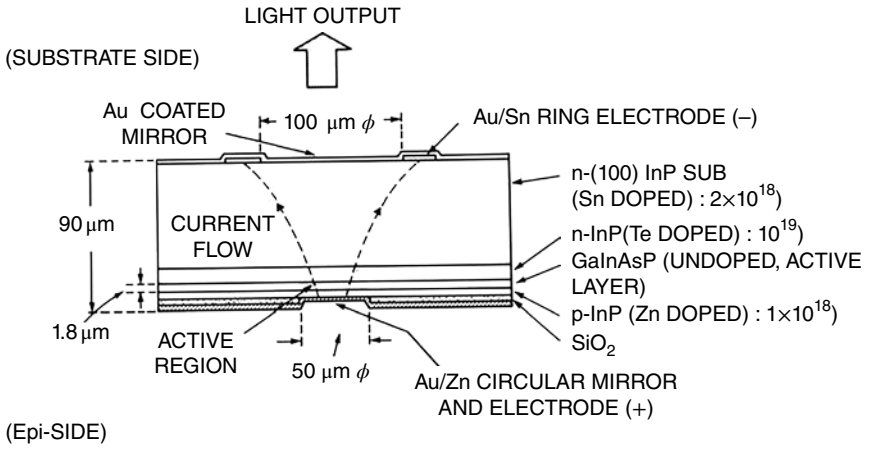

Figure 1.14 The first demonstration of a surface-emitting laser. *Source:* Figure by K. Iga [29] [copyright reserved by author].

screen). In the first stage, Ia, there were many technical challenges to overcome to realize this new device. The main challenges were the relatively low optical gain, overall mirror quality, and efficient current injection.

The first device (prototype) was realized in 1979 using a GaInAsP-InP material for the active region. The VCSEL operated at a 1300 nm wavelength [29]; a schematic cross section of the device is shown in Figure 1.14. This VCSEL used a double heterostructure with GaInAsP as an active layer, which was grown on an InP substrate. Light is emitted by injecting current from circular electrodes, and metal reflectors are formed above and below the substrate to form a resonator. This laser was driven by a pulsed current and was cooled to 77 K using liquid nitrogen. At 800 mA the device lased. When we looked at the light coming out of the device, it flashed rapidly at a certain current. It was possible to finally measure the spectrum, and it was much narrower than LEDs, which indicated laser oscillation. As mentioned above, the device was named surface-emitting laser. The threshold was very high, more than 20 times that of a normal laser, and as such, the device was out of order immediately!

1.3.1.2 Stage Ib: First Room-Temperature Continuous-Wave Operation

In 1982, Iga and co-workers made a VCSEL with 10 μm length cavity and confirmed the clear VCSEL oscillation [30]. In 1982, Iga's group made a buried confinement VCSEL with a 6 mA threshold GaAs device using liquid phase epitaxy (LPE) [31]. A major breakthrough was the achievement of continuous-wave (CW) operation at room temperature (RT) at 820 nm wavelength on GaAs substrate by Iga and Koyama (also from Tokyo Institute of Technology) in 1988 [32, 33]. The device structure is shown in Figure 1.15(a). The device was grown by metal organic chemical vapor deposition (MOCVD). With this achievement, global R&D of VCSELs has outperformed ordinary semiconductor lasers in the area of expertise. The concept of semiconductor DBR demonstration in 1988 [34] and the introduction of multi-quantum wells into VCSEL [35] contributed to the improvement of VCSEL development in later years.

After this breakthrough from Tokyo Institute of Technology, continuous room-temperature operation of the VCSEL, as shown in Figure 1.15(b), was also achieved by Jack Jewell and co-workers at Bell Laboratories in 1989 [36, 37]. The concept of periodic gain or matched gain in quantum wells contributed to reduce the threshold by Larry Coldren and co-workers [38, 39].

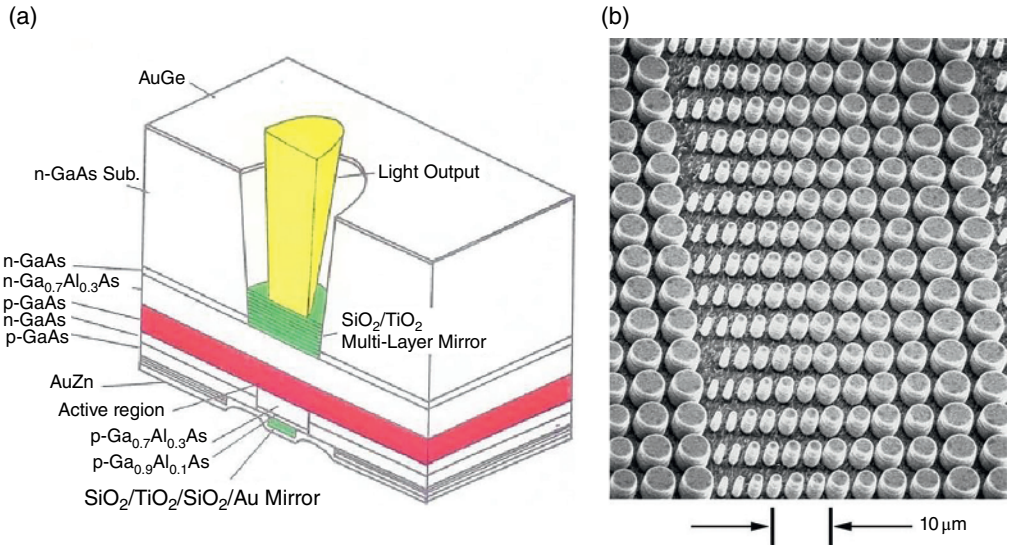

Figure 1.15 Initial VCSELs achieving room-temperature continuous operation. (a) The VCSEL device that exhibited the first room-temperature continuous-wave operation by Koyama and Iga in 1988 [32]. *Source:* Copyright reserved by Fumio Koyama and Kenichi Iga (b) A 2D micro-post array by Jewell and Lee in 1989 [36, 37]. *Source:* Adapted from IEEE.

1.3.2 Stage-II: Spread of Worldwide R&D

The second stage (1991–2000) covers the expansion of VCSEL research, the advancement in growth technology, and the emerging application needs in data communications. The first DARPA funding was driven by the Joint Strike Fighter (JSF) program. Three centers for optoelectronics were started in universities. Honeywell, Motorola, and HP were the primary companies working on the programs. More details can be found in the wiki page:

https://en.wikipedia.org/wiki/Vertical-cavity_surface-emitting_laser.

Areas of emphasis in Stage II include mass production technology [40], threshold current reduction[39–42], transverse mode control, oxidation [43, 44], polarization control, initial tunable VCSELs [45], MEMS elements [46], 2D arrays [47], high-speed and high-power VCSELs, InP-based device with continuous operation [48] and quantum wells VCSELs, and so on. This was a golden period in the VCSEL journey to mass production, and many technical and manufacturing advances contributed to the foundation of VCSEL technology.

1.3.3 Stage III: Extension of Applications and Initial Commercialization

Stage-III of VCSEL development started in 1999, shown in Figure 1.12, as we entered a new information and technology era in 2000. The third stage (1999–2010) brought on new development of wavelengths, single mode, VCSEL arrays, volume manufacturing driven by Internet traffic demand, autofocus, and so forth, and the focus has shifted to commercial efforts. Why did 1310–1550 nm VCSELs not become widely adopted? That was primarily due to the technical difficulty of making mirrors and overcoming optical loss in materials.

In 2000 one of the authors (Iga) wrote a VCSEL review paper [49] and in the same special issue, DARPA managers Elias Towe, Robert F. Leheny, and Andrew Yang wrote the following about VCSEL in their review paper [50]: “Its size, manufacturability, and potential ease of heterogeneous

integration of electronics promise a range of applications that have yet to be explored." This was the time when DARPA invested considerable human and monetary resources in the R&D of VCSEL, in particular the massive integration of VCSELs, detectors, micro-optics and driving electronics for free-space optical interconnects and all optical switching. However, practical and commercial free-space interconnect and all optical switching did not really pick up during the subsequent years. This investment nonetheless continued to drive VCSEL innovations such as high-power VCSEL arrays, high-contrast gratings, athermal VCSELs, coupled cavity VCSELs, VCSELs-based slow light waveguide devices, multi-wavelength VCSELs/WDM [51], quantum dot VCSELs, high-bandwidth VCSELs (>20 GHz), and so forth.

VCSELs are currently applied in various optical systems, such as optical networks, parallel optical interconnects, laser printers, computer mice, and so on. The three critical application areas that provided the commercial impetus for continued VCSEL expansion were high-speed data connectivity, computer mice, and laser printing.

1.3.3.1 LAN for Internet

A first large market for VCSELs with large-scale production had begun in 1995 [40]. Around 1999, the Internet spread rapidly worldwide. The dramatic growth of data centers created communication networks that support the Internet, including long-distance optical fiber networks and local area networks (LANs). Metaphorically, the artery of the blood vessel is the long-distance line, and the LAN is a capillary. VCSEL was adopted as a light source for LANs operating at 1 Gbit/s and running Fiber Channel and Ethernet protocols.

The protocols were further standardized (10G; IEEE802.3ae in 2002, 100G; IEEE802.3ba in 2011) for the optical fiber communication that constitutes the LAN of the Internet. In 2020, high speed VCSELs and the pulse amplitude modulation (PAM) scheme have been developed for 400 Gbit/s high-speed Ethernet. Information flows through the capillaries of companies and universities. Details on VCSELs in data communications will be covered in Chapter 4.

In addition to applications in data centers owned and operated by IT companies, national organizations and universities began to include optical interconnects in computing architectures. For the supercomputer TSUBAME 3.0 by Tokyo Institute of Technology more than 16 000 VCSELs were included in the system. More than 300 000 VCSELs are used in IBM's top supercomputer. In the world's fastest (2019 and 2020) supercomputer Fugaku of RIKEN of Japan, it was reported that the numbers of VCSEL chips used was 640 000.

https://www.r-ccs.riken.jp/en/fugaku/project/outline.
https://www.fujitsu.com/downloads/SUPER/primehpc-fx1000-hard-en.pdf.

1.3.3.2 Computer Mouse

A computer is one way to access the Internet, and a computer mouse is useful for operating a computer. Since around the year 2000, VCSELs have also been applied to computer mice by Hewlett-Packard; this represented the first high volume use of VCSELs in a consumer market. The use of VCSELs in consumer electronics may be comparable to the development of electronic devices such as LSIs and semiconductor memories. VCSELs used in computer mice will be further discussed in Chapter 8.

1.3.3.3 Laser Printers

VCSEL arrays were introduced into laser printers in 2001 by companies such as Fuji Xerox, Ricoh, and Canon/Sony. Since then, VCSELs have largely replaced edge-emitting lasers and LEDs in printers. The aforementioned companies have about 80% market share of integrated laser printers in the world. VCSELs in laser printing will be further discussed in Chapter 8.

1.3.4 Stage IV: Spread of VCSEL Photonics

In the fourth stage of VCSEL history, from 2010 to 2020, the true scaling of VCSEL production has been realized. In data communication, highly reliable 850 nm VCSELs are made using InGaAs quantum wells with 3 dB bandwidths exceeding 25 GHz and operated above 70 Gb/s NRZ. New modulation (PAM-4) standards are made for higher speeds to meet the continued network demand. This is also supported by development of short wavelength WDM VCSELs (in the 850–980 nm band).

In the optical sensing area, high-power 940 nm VCSELs arrays have been made with optimized designs with power conversion efficiency > 50%, slope efficiency = 1.0 W/A, and with new trends of using multi-tunnel junctions that offer a power conversion efficiency > 60%, slope efficiency = 3.0 W/A, with power densities of 1 kW/mm^2. This facilitated the use of VCSEL arrays in consumer devices (mobile/smart phones/smart homes), infrastructure and transport applications incorporating LiDAR, surveillance and night vision products, robots, drones, IoT, and so on. Further applications include multi-mode VCSEL arrays in LiDARs at 905 nm, 850 nm, and 1060 nm; large-scale 940 nm arrays in industrial heating systems. On the other hand, single-mode VCSELs are being applied to optical coherence tomography (1060 nm) and atomic clocks. Details and references can be found in related chapters.

The multi-function ability of VCSELs further expanded manufacturing bases across the world with investments prompting high market demands never seen before. This also triggered high-volume manufacturing from 4″ (100 mm) to 6″ (150 mm) for optical sensor products. All these items will be discussed in Chapters 3–9.

1.3.5 Stage V: VCSEL Industry

In the fifth stage (2020 onward) VCSELs will continue to expand in global volume production and find new application areas. The ever-increasing demand for data communication and emerging technologies in machine vision, artificial intelligence (AI), augmented reality (AR), mixed reality (MR), and the Internet of Things (IoT) will drive global demand for VCSELs [52]. In this stage, VCSELs will affect nearly all aspects of human life. Details on computer vision (AR, MR, VR) will be introduced in Chapter 5. The application to automotive LiDARs and autonomous shuttles will be covered in Chapter 6.

1.4 Timeline and Milestones

1.4.1 Milestones of VCSEL Research and Development

In Table 1.2 we show a list of key benchmark events based on 44 years of basic research and commercial product developments on semiconductor lasers and VCSELs.

1.4.2 Single-Mode and Multi-Mode Behavior

Semiconductor lasers oscillate in different modes (power radiation patterns) that depend on the dimensions of the optical resonator. Especially for VCSELs, the mode structure or pattern depends on the size and shape of the oxide aperture (mode) diameter used for current and optical confinement [53, 54]. Several kinds of modes appear in the emission spectra, namely longitudinal, transverse, single, and multi-modes. In Figure 1.16 we show how the behavior of VCSEL in single longitudinal and multi-transverse (and longitudinal) operation. More details on the VCSEL mode structure will be discussed in Chapter 2.

Table 1.2 Milestones of surface emitting laser research and development.

1977	Surface-emitting laser concept proposed
1979	First device demonstrated (77 K, pulsed)
1988	First RT CW operation
1988	Semiconductor DBR
1989	QW VCSEL
1989	Micro-post QW laser RT CW (Bell Labs)
1989	Periodic gain proposed (UCSB)
1990	AlGaAs hydro-oxidization (UIUC)
1992	VCSEL mechanical tuning demonstrated
1995-	Low threshold device competition $I_{th} < 0.1$ mA
1995	MEMS tunable VCSEL (USB)
1996	VCSEL commercialization (Honeywell)
1999	VCSEL LAN
2000	Oxide aperture device reliability
2001	VCSEL printer (Fuji, Xerox),
2001	Computer mouse (HP)
2002	10G Ethernet standard IEEE802.3ae
2003	4Gb/s VCSELs (Honeywell)
2006	High-contrast grating for VCSEL (UC Berkeley)
2010	100G Ethernet standard IEEE802.3ba
2011-	VCSEL photonics
2016	VCSEL arrays for sensing
2016	VCSEL SWDM in datacom
2017	VCSEL face ID 3D sensor (iPhone X from Apple)
2018	400G AOC (Finisar/II–VI)
2020	LiDAR scanner (iPhone 12 Pro, iPad Pro 11″/12″ from Apple)
2021-	VCSEL Industry

Italic: From K. Iga's group.
RT CW: Room-temperature continuous wave
QW: Quantum well.

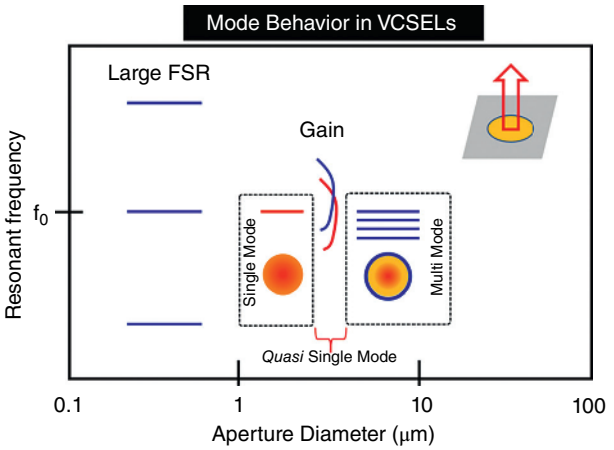

Figure 1.16 Origin of single-mode and multi-mode behavior in VCSELs. *Source:* [55, 8]. Figure by K. Iga [copyright reserved by author].

The origin of multi-mode operation in a VCSEL is not from longitudinal mode behavior but multiple transverse mode oscillation. When the lateral extent of the optical resonator diameter is extended to larger than several microns, multi-transverse with multispectral-mode operation is achieved. On the other hand, small diameters lead to single-transverse and single spectral-mode operation.

1.4.3 Major Features of VCSELs

VCSELs have become the light source of choice for many applications and are rapidly replacing edge-emitting lasers (EELs) and LEDs in many more every day. The inherent advantages in manufacturing and the ability to tailor the VCSEL properties to different applications has been key to their success. The ability to scale the optical power and emission pattern with 2D arrays of emitters has enabled the widespread adoption of 3D sensors. Table 1.3 summarizes the typical operating characteristics of VCSELs and EELs. Even with the long list of advantages, there are still many applications where EELs offer a better solution. Some areas where EELs are still dominant are single-mode fiber optic communications and extremely high-power applications.

The authors rearranged Table 1.3 to provide a simple picture of advantageous and key characteristics along with performance attributes into Table 1.4.

1.4.4 VCSELs as Major Optical Components

The single-mode and multi-mode VCSELs categorized in Section 1.2.1 show decisive advantages as optical components in communication and sensing as shown in Table 1.5.

i) Single or 1D VCSEL emitters are used as light source in active optical cable (AOC) or optical interconnects for data communication.
ii) 2D VCSEL arrays found high volume applications as printer and time of flight (ToF) or structured light sources in 3D sensing. Proximity illumination in Face Recognition (FR), Gesture Recognition (GR). Time-of-Flight (ToF), Phase shift, FMCW light sources in 3D ranging. They are also used for scanning mode or flash mode LiDARs for automotive, surveillance/night vision ranging, robotics, and drones.
iii) Large scale VCSEL arrays in industrial heating etc.

All these items will be discussed in detail in Chapters 4–9 as classified in Table 1.5.

1.4.5 VCSELs in Optical Communication and Sensing

1.4.5.1 The Concept of VCSEL Communication and Sensing

As depicted in Figure 1.16, in most of the applications, VCSELs are used either as light transmitters for communication or light sources for sensors. Data transmission in optical communication systems requires a light transmitter and a receiver together with a transmission media such as optical fibers or air. Along with these core components, driver/receiver ICs with connecting optics are incorporated.

Similarly, in an optical sensing system, a VCSEL light source illuminates 2D/3D objects, and a receiver is used to capture the reflected rays from the objects. Figure 1.17 shows the concepts of optical communication and sensing that are required to understand Chapters 4–9.

1.4.5.2 VCSELs in Optical Communications

The two-way communication concept described in Figure 1.16(a) is used in optical transceivers made from VCSELs, such as pluggable transceiver, active optical cable (AOC), HDMI-AOC, active direct attach copper (DAC), and USB-3 or USB-C. These are high-volume applications especially in 100 and 400 Gb/s networks in data centers with ranges from <3 m to >100 m. Normally,

Table 1.3 Differences between VCSEL and edge-emitting lasers (EEL).

			VCSEL			Edge-Emitting Lasers	
	Structure/Parameter	**Units**	**Single Mode**	**Multi-Mode**	**Multi-Mode Array**	**DFB/DBR**	**Fabry-Pérot**
Electro-Optical	Operating current	mA	6 mA		depends on the numbers of emitters	30 mA	
	Threshold current	mA	<1 mA			25 mA	
	Series resistance	ohm	50 Ω			3 Ω	
	PCE/WPE	%	35–40%		>40%	>50%	>55%
	Slope efficiency	Watt/Amp	0.4–0.7 W/A		>0.45 W/A	0.3 W/A	
	Output power	mW	1–10 mW		>1000 mW	<120 mW	
	Rise and fall time	nano sec	<1 ns			5–10 ns	
	Modulation speed	Gbit/s	>40 Gb/s	>200 Gb/s	not reported	>200 Gb/s	>25 Gb/s
	3 dB down S21 bandwidth	GHz	>20 GHz	>40 GHz	not reported	> ~ 100 GHz	>30 GHz
Spectrum	Linewidth	nm	<0.1 nm	0.2–0.6 nm	1–3 nm	<1 nm	1–2 nm
	Beam divergence (angle)/ quality	degree	symmetric (2–20°)/no astigmatism			elliptical (15/40°)/ astigmatism	
	Speckle	looking	high	low	moderate	high	
	Single/multi-mode behavior	looking	pure single		multi-transverse	quasi-single/ multi-longitudinal	
Thermal	Wavelength stability (shift)	nm/Kelvin	0.06 nm/K			0.3 nm/K	0.3
	Reliability (lifetime)	hours	high			high	
Manufacture	Array scaling	dimension	2D			1D	
	Wafer diameter	inch(mm)	4″ (100 mm) & 6″ (15O mm) ready			4″ (100 mm) to be ready	
	Assembly and packaging	complexity	simple and easy 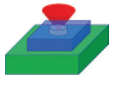			**complex** 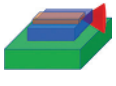	
	Growth and processing	complexity	monolithic/standard CMOS			regrowth/facet coating needed	
	Cost	amount	low			high	

Source: [Table by B. D. Padullaparthi and K. Iga] [copyright reserved by authors].

Table 1.4 Attributes of VCSEL in datacom, sensing, and manufacturing.

Datacom	Sensing	Manufacturing	Others (Performance)
high fiber coupling efficiency	high peak pulse powers	vertical integration	low threshold currents
high bandwidths	high PCE and SE	array scalability and small footprint	circular beam (Low divergence)
high modulation speed	high rise and fall time (integration time)	easy alignment and packaging	narrow linewidth
low power consumption (energy efficient in data centers)	low power consumption (long battery operating times consumer)	monolithic process handling (epi-growth and wafer fabrication)	operation in single-mode and multi-mode
wavelength tunability (WDM)	high beam quality	low cost and high yield	high reliability (auto grade)
low thermal impedance (efficient heat dissipation)		on-wafer testing	wavelength stability

Source: [Table by B. D. Padullaparthi and K. Iga] [copyright reserved by authors].

Table 1.5 Mode dependent VCSEL applications.

	Optical Communications	Optical Sensing	Others
Single mode	mid distance transceiver	optical mouse	printers
		gas sensing	displays
		OCT	atomic clock
		bio sensing	
		motion sensing	
Multi-Mode	LAN		
	short-reach transceiver	face recognition	manufacturing
	interconnects	illumination	heating
		LiDAR	
		robotics	

Source: [Arranged by K. Iga and B. D. Padullaparthi] [copyright reserved by authors].

multi-mode fibers are used for short-reach (<100 m) applications, and single-mode fibers are employed for long-reach (2–10 km) applications.

Using high performance VCSELs with sufficient output power, low-loss optical fibers, and efficient high-speed detectors, data can be transmitted at speeds of 25–100 Gb/s over 300 m at temperatures well over 85°C [56]. The details of multi-mode VCSELs for data communications/data-center applications are discussed in Chapter 4.

1.4.5.3 VCSELs in Optical Sensing

Referring to the optical sensing system in Figure 1.16(b), short-range (<10 m) image sensing in consumer electronics use 2D VCSEL arrays as light source with two different schemes. In the first scheme, intense uniform light from 2D VCSEL arrays illuminates on an 2D/3D object, is reflected

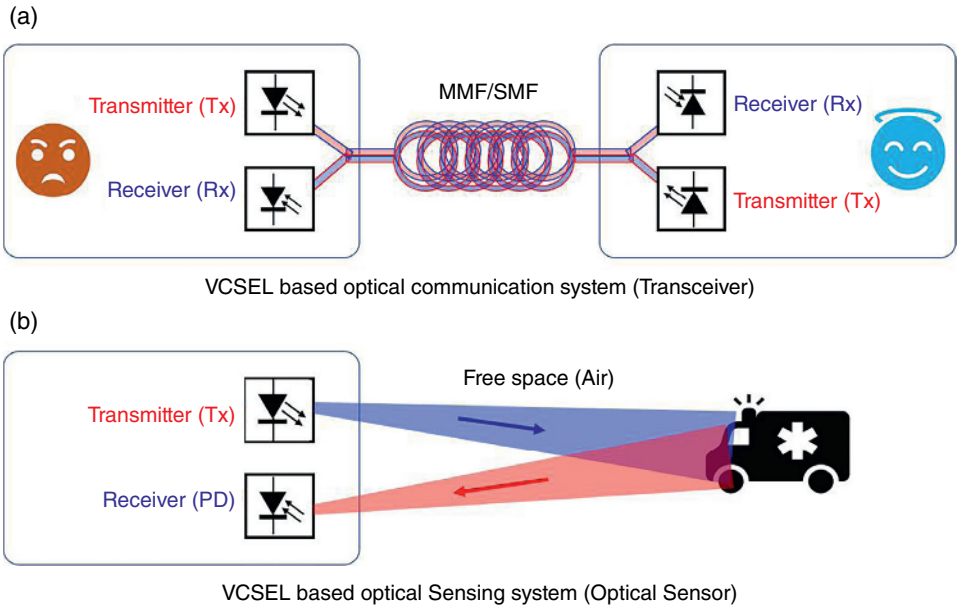

Figure 1.17 VCSEL-based optical communication and sensing systems. *Source:* Figure by K. Iga [copyright reserved by author].

back to image sensors, and the distance of the object is measured by a method called time of flight (ToF).

Besides, a simple 3–6-emitter VCSEL array is also used for proximity sensing in smart phones using the ToF technique.

In the second scheme, intense distributed light from a 2D VCSEL array illuminated on a 3D object is reflected back to the image sensors, and the depth of the object is measured by a method called structured light. This is the mechanism of face unlocking in smart phones. There are a host of emerging applications from VCSEL arrays as sensors in AR, robotics, smart-home appliances, and so on. Details are discussed in Chapter 5.

Long-distance ranging or object detection (~250 m or longer) can also be done using the sensing concept shown in Figure 1.16 for automobile by using LiDARs. This is sometimes known as vehicle-to-everything (V2X). LiDARs use individually or row/column addressable arrays of VCSELs or edge-emitting laser arrays to illuminate the scene either through a single flash, sequential flashes by selectively addressing the emitters, or scan functions, and the object image is created through powerful signal processing and artificial intelligence (AI).

Besides ToF, more precise object measurement techniques such as optical phased arrays (OPA) or frequency modulations (FMCW) are also used for advanced driver-assistance systems (ADAS). Details of other applications are discussed in Chapters 6–9.

To facilitate comprehension, supplementary information is given as appendices on generic VCSEL design (Appendix A), epitaxial growth (Appendix B), wafer processing (Appendix C), testing (Appendix D), reliability and qualification (Appendix E), and eye-safety issues (Appendix F). Special notes on display (Appendix G), red VCSELs (Appendix H), photodetectors (Appendix J), and GaN VCSELs (Appendix I) and are also provided.

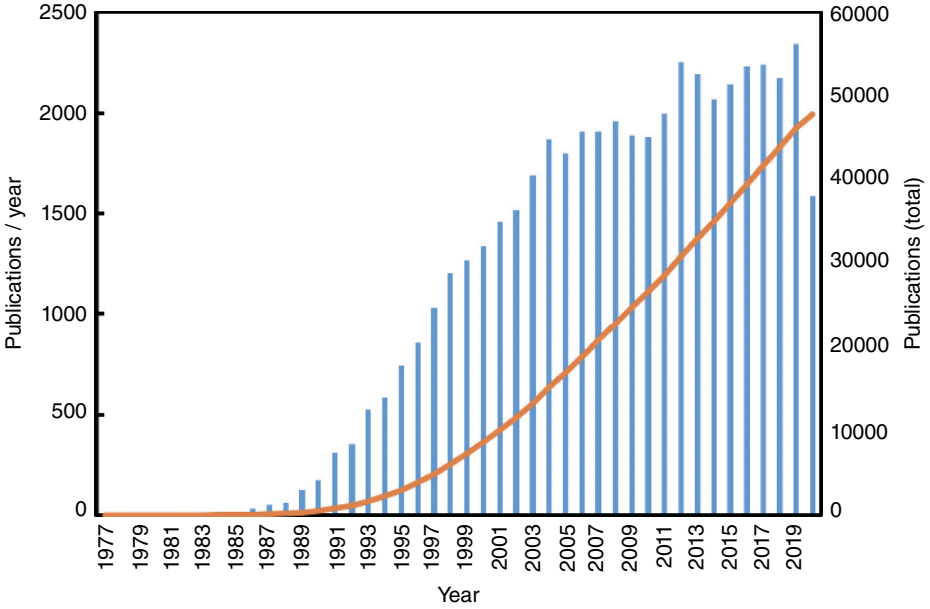

Figure 1.18 Published papers on VCSEL. *Source:* Data taken from Google Scholar on November 2, 2020. (Searching key words: "VCSEL" OR "vertical-cavity surface-emitting laser" OR "surface emitting laser" in the text or title.) [Image courtesy of Tomoyuki Miyamoto, Tokyo Institute of Technology.]

1.5 State of VCSEL Development

1.5.1 Published Papers

Figure 1.18 shows the number of published papers per year and accumulated statistics. Note that the total number of related papers has reached about 50,000 as of 2020. The yearly publications have skyrocketed over the last decade, indicating that commercialization is taking place.

1.5.2 Toward VCSEL Photonics

Ever since Honeywell started VCSEL commercialization and introduced the first reliable product in around 1996 [57], VCSEL technology has made a huge impact on several key industries with multiple growth windows. Thanks to several commercial epi-houses, III-V opto-foundries, and other equipment vendors, researchers and engineers have overcome great challenges to make VCSEL-based commercial products a practical reality since the beginning of 2021.

After 44 years of VCSEL invention [25] and the marathon industry efforts to realize volume manufacturing, it is not surprising that most people carry a VCSEL device along with them, if not a few! This means VCSELs have rapidly grown up, fully matured, and penetrated into commercial products that affect the daily lives of humans.

Four major industries dominate most of the VCSEL applications space (called core products), while few other neighboring fields are also emerging in the entire VCSEL application seabed. On core applications, the first is high-speed VCSELs for data communications and data center applications. There is a steady demand for 100 to 300 m active optical cables in 100–400 Gb/s data center

needs, HDMI AOC, USB-3 (c-type), and so on. The world's fastest (as of 2019 and 2020) high-performance computer, Fugaku, uses more than 6 400 000 chips of VCSELs for AOCs.

The second and biggest opportunity is high-power VCSEL arrays for consumer electronics (3D sensing and imaging up to 10 m), including illumination, face recognition (FR), and augmented reality (AR) needs. This extends to object detection for autonomous vehicles and intelligent transport through powerful long-range LiDARs up to 250 m or beyond. Further high-power VCSEL arrays (where 100 000 to a few million units of emitters are needed) find applications in industrial heating.

Furthermore, we find VCSEL applications in neighboring areas such as coherent communication, laser printers, additive manufacturing, gas sensing and spectroscopy, biometrics such as optical coherence tomography (OCT) and iris scans, gaming (VR and MR), robotics, and drones attracting considerable investments, particularly on AI programming, smart home and IoT, and automotive Ethernet and even to quantum computing.

1.5.3 Toward VCSEL High-Volume Manufacturing

The proliferation of VCSELs into several industries and their use in countless commercial products make the VCSEL industry bright and vibrant. In Figure 1.19 we show the market of VCSELs estimated in 2021. It is quite amazing to realize that hundreds of millions of VCSELs have been deployed. The overall market is forecast to continue to grow in current core applications, and it is expected that even more areas will be uncovered to edge areas in the future. The large shipping volume has created an ecosystem of vertically integrated manufacturers as well as robust foundry vendors. With millions of epi-wafers processed, multibillion-dollar market forecasts, and nearly a trillion of VSCEL units shipped, undoubtedly VCSELs are the future optical components of choice and are cementing their presence in the photonics industry!

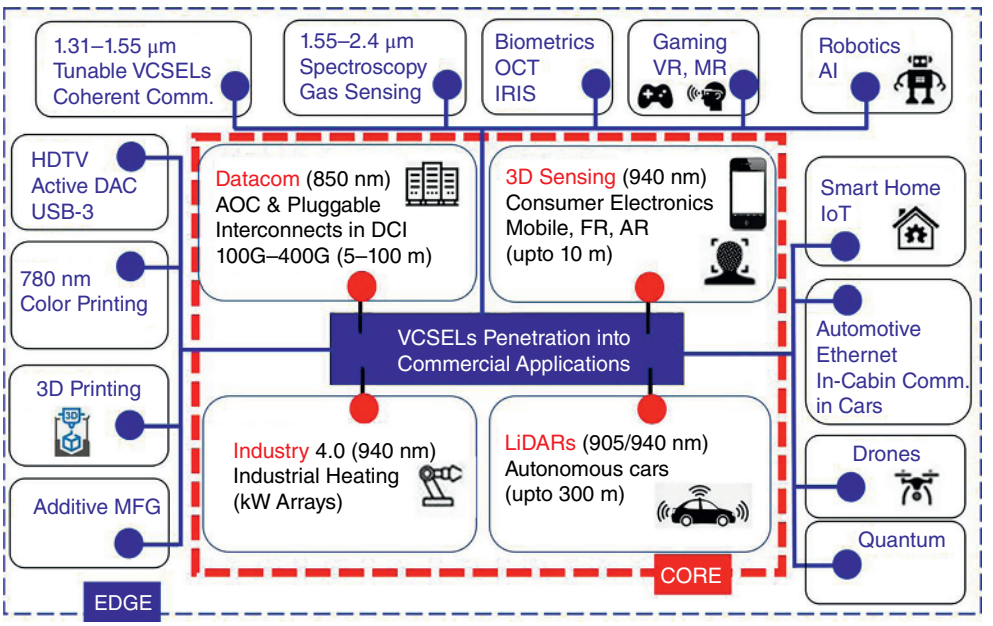

Figure 1.19 Application fields of VCSEL market as of 2021; data taken from various sources. *Source:* Figure by B. D. Padullaparthi and K. Iga [copyright reserved by authors].

In Figure 1.20, we show a modified hype cycle of VCSEL industrialization. This shows the timeline of VCSEL industrialization based on Iga's personal limited knowledge. In Chapter 10, we will discuss this matter after reviewing all the items in technical chapters by all the authors and editor by including other applications.

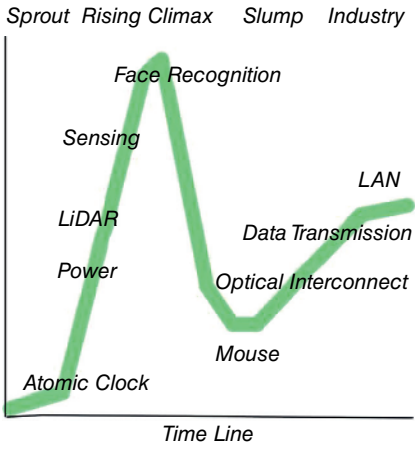

Figure 1.20 The modified hype cycle of VCSEL industrialization. *Source:* K. Iga's observation in the middle of 2020 [copyright reserved by author].

1.5.4 Prospects of VCSEL Market

At the beginning of 2021, VCSEL technology has emerged as a low-cost, high-volume business opportunity for large-scale manufacturers, comparable to other semiconductor technologies such as GaN, SiC RF, and power devices, LEDs, displays, photovoltaic solar cells, Si-photonics, and InP-based semiconductor lasers. A schematic of market sizes for different VCSEL technologies are shown in Figure 1.21. The total photonics market is expected to reach about $80 billion by 2025 from $24 billion in 2020. The authors consider two types of opportunities for VCSEL-based commercial products, namely **core** and **edge** markets.

The **core** market includes four major areas: datacom, 3D sensing (mobile), 3D imaging LiDAR (automotive), and industrial heating. In these areas, VCSEL is a proven technology addressing strong societal needs and appears to be gaining a major market share with readily available commercial products.

The **edge** markets include defense and aerospace, medical (OCT and iris scans), gas sensing, gaming, global AR/VR/MR, surveillance (IP and CCTV cameras), 3D printing, laser printing, and many other applications. Other **edge** markets such as robotics, AI, and smart-home appliances

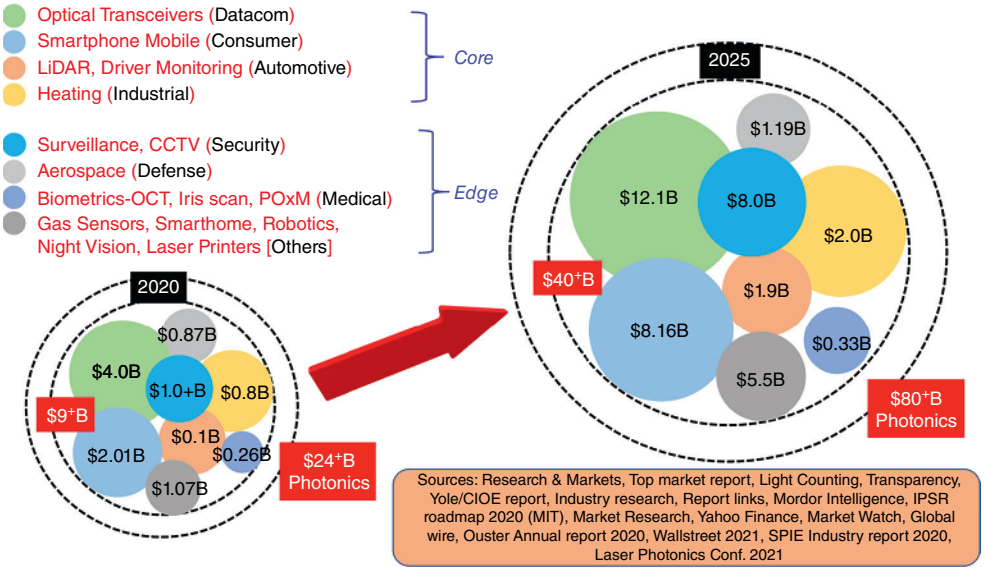

Figure 1.21 Total addressable market of VCSELs at module levels till 2025. *Source:* B. D. Padullaparthi [copyright reserved by author].

either have small market share or are still developing prototypes for final stages of release for commercial products [58].

The total addressable market projected for VCSEL's **core** and **edge** areas at module level is expected to be around $40 billion by 2025, where the **core** part alone is forecast to be about a $24 billion by 2025 market, as shown in Figure 1.20.

The chip level projection for datacom, telecom, mobile consumer, automotive, medical, industrial, and defense fields is estimated to be about $4.8 billion by 2025, that is 24% of the corresponding module level projections.

With an increasing number of autonomous cars with LiDARs by 2030, it is anticipated that the market size of the automotive industry will exceed that of consumer electronics, prompting a large number of VCSELs to be used for long-distance ranging as flash or scan LiDARs. Further, several **edge** and other markets projected a total reaching $80 billion. When a fraction of 15% (about $8.4 billion) is assumed for add value to **core** fields, the total addressable market size at module level will be at least about $32.4 B, as shown in Figure 1.20. Some chip level details are given in Chapter 3.

In summary, it is concluded that VCSEL is finding a vibrant commercial prospect for high-volume manufacturing and product demands that are further expanding.

References

1 T. H. Maiman, "Stimulated optical radiation in ruby," *Nature*, **187** 4736, pp. 493–494 (1960).

2 R. N. Hall, G. E. Fenner, J. D. Kingsley, T. J. Soltys and R. O. Carlson, "Coherent light emission from GaAs junctions," *Phys. Rev. Lett.*, Vol. **9**, No. 9, pp. 366–368 (1962).

3 T. M. Quist, R. H. Rediker, R. J. Keyes, W. E. Krag, B. Lax, A. L. McWhorter and H. J. Zeigler, "Semiconductor maser of GaAs," *Appl. Phys. Lett.*, Vol. **1**, No. 4, pp. 91–92 (1962).

4 M. I. Nathan, W. P. Dumke, G. Burns, F. H. Dill, Jr. and G. Lasher, "Stimulated emission of radiation from GaAs p-n junctions," *Appl. Phys. Lett.* Vol. **1**, No. 3, pp. 62–64 (1962).

5 N. Holonyak, Jr. and S. F. Bevacqua, "Coherent (visible) light emission from $Ga(As_{1-x}P_x)$ junctions," *Appl. Phys. Lett.*, Vol. **1**, No. 4, pp. 82–83 (1962).

6 I. Hayashi, P.B. Panish, P.W. Foy and S. Sumski, "Junction lasers which operate continuously at room temperature," *Appl. Phys. Lett.*, Vol. **17**, pp. 109–111 (1970).

7 Zh. I. Alferov, V. M. Andreev, E. L. Portnoi and M. K. Trukan, "AlAs-GaAs heterojunction injection lasers with a low room-temperature threshold," *Fiz. Tekh. Poluprovodn.*, Vol. **3**, pp. 1328–1332 (1969); Sov. Phys. Semicond., Vol. 3, pp. 1107–1110 (1970).

8 K. Iga and G. Hatakoshi, "Treasure Microbox of Optoelectronics," Adcom-Media Co. Ltd. Tokyo, April 25, 2020. (PDF Japanese language version).

9 H. Kroemer, "A proposed class of heterojunction injection lasers," *Proc. IEEE*, Vol. **51**, No. 12, pp. 1782–1783 (1963) H. Kroemer: "Solid state radiation emitters," US Patent 3309553 (Application date: Aug. 16, 1963).

10 Y. Suematsu and K. Iga, "*Introduction of Optical Fiber Communication*," John Wiley and sons, 1976.

11 H. C. Casey and M. B. Panish, *Heterostructure Lasers*, Academic Press, New York (1978).

12 A. Yariv: Optical Electronics, 1991.

13 L. A. Coldren, S. Corzine, and M. L. Masanovic, "*Diode Lasers and Integrated Optics*," Wiley, 1994.

14 S. L. Chuang, "*Physics of Optoelectronic Devices*," John Wiley & Sons, New York, 1995.

15 J.P. van der Ziel, R. Dingle, R.C. Miller, W. Wiegman and W.A. Nordland, Jr., "Laser oscillation from quantum states, in very thin GaAs-$Al_{0.2}Ga_{0.8}As$ multilayer structures," *Appl. Phys. Lett.*, Vol. **26**, No. 8, pp. 463–465, 1975.

16 Y. Arakawa and A. Yariv, "Theory of gain, modulation response and spectral linewidth in AlGaAs quantum well lasers," *IEEE J. Quantum Electron.*, Vol. **QE-21**, No. 10, pp. 1666–1674, Oct. 1985.

17 M. Asada, Y. Miyamoto and Y. Suematsu, "Gain and the threshold of three-dimensional quantum-box lasers," *IEEE J. Quantum Electron.*, Vol. **QE-22**, pp. 1915–1921, 1986.

18 K. Iga, "*Fundamentals of Laser Optics*," Plenum, p. 173, (1994).

19 M. Asada and Y. Suematsu, IEEE J. QE, vol. QE-21, p. 434(1985).

20 H. Kogelnik and C.V. Shank, "Coupled wave theory of distributed feedback lasers," *J. Appl. Phys.*, Vol. **43**, No. 5, pp. 2327–2335, May 1972.

21 Y. Suematsu and K. Hayashi, "General analysis of distributed Bragg reflector and laser resonator using it," *National Conv. Inst. Electron. Comm. Eng*, **1200**, p. 1203, (July 25–27, 1974).

22 W. Tsang and S. Wang, "GaAs-$Ga_{1-x}Al_xAs$ double-heterostructure injection lasers with distributed Bragg reflectors," 9th IQEC, p. 38 June 1976.

23 K. Utaka, Y. Suematsu, K. Kobayashi and H. Kawanishi, "GaInAsP/InP integrated twin-guide lasers with first-order distributed Bragg reflectors at 1.3μm wavelength," *Jpn. J. Appl. Phys.*, Vol. **19**, No. 2, pp. L137–L140, Feb. 1980.

24 Y. Suematsu, "Dynamic single mode lasers," *J. Lightwave Technol.*, vol. **32**, no. 6, pp. 1144–1158, March 2014.

25 K. Iga, Research Notebook, March 22, 1977.

26 K. Iga, T. Kambayashi, C. Kitahara, "Surface-emitting GaInAsP / InP laser (I)," 25th Joint Conference on Applied Physics (at Musashi Institute of Technology), 27-p-11, p. 63, March 27, 1978.

27 K. Iga, Y. Suematsu, K. Kishino and H. Soda, "Surface emitting semiconductor laser," Japan. Patent, Hei 1-56547, Jan. (1980).

28 K. Iga and G. Hatakoshi, "The Principle and Application Systems of Vertical Cavity Surface Emitting Laser," Adcom-Media Co. Ltd. Tokyo, Sept. 25, 2020. (PDF Japanese language version)

29 H. Soda, K. Iga, C. Kitahara, and Y. Suematsu, "GaInAsP/InP surface emitting injection lasers," *Jpn. J. Appl. Phys.*, vol. **18**, no. 12, pp. 2329–2330 (1979).

30 Y. Motegi, H. Soda, and K. Iga, "Surface emitting GaInAsP/InP injection laser with short cavity length," *Electron. Lett.*, Vol. **18**, No. 11, pp. 461–463 (1982).

31 K. Iga, S. Kinoshita, and F. Koyama, "Microcavity GaAlAs/GaAs surface-emitting laser with I_{th}=6 mA," *Electron. Lett.*, vol. **23**, no. 3, pp. 134–136, Jan. (1987).

32 F. Koyama, S. Kinoshita, and K. Iga, "Room temperature cw operation of GaAs vertical cavity surface emitting laser," *Trans. IEICE*, vol. **E71**, No. 11, pp. 1089–1090 (1988).

33 F. Koyama, S. Kinoshita, and K. Iga: "Room-temperature continuous wave lasing characteristics of GaAs vertical cavity surface-emitting laser," *Appl. Phys. Lett.* vol. **55**, no. 3, pp. 221–222 (1989).

34 T. Sakaguchi, F. Koyama, and K. Iga, "Vertical cavity surface-emitting laser with an AlGaAs/AlAs Bragg reflector," *Electron. Lett.*, vol. **24**, no. 15, pp. 928–929, July (1988).

35 H. Uenohara, F. Koyama, and K. Iga: "Application of the multiquantum well (MQW) to a surface emitting laser," *Jpn. J. Appl. Phys.*, vol. **28**, no. 4, pp. 740–741, April (1989).

36 J. L. Jewell, S. L. McCall, A. Scherer, H. H. Houh, N. A. Whitaker, A. C. Gossard, and J. H. English, "Transverse modes, waveguide dispersion and 30 ps recovery in submicron GaAs/AlAs micro-resonators," *Appl. Phys. Lett.* vol. **55**, no. 1, pp. 22–24 (1989).

37 Y. H. Lee, J. L. Jewell, A. Scherer, S. L. McCall, J. P. Harbison, and L. T. Florez: "Room- temperature continuous-wave vertical-cavity single-quantum-well micro-laser diodes," *Electron. Lett.*, vol. **25**, no. 20, pp. 1377–1378 (1989).

38 S. W. Corzine, R. S. Geels, R. H. Yan, J. W. Scott, and L. A. Coldren, "Efficient, narrow-linewidth distributed-Bragg reflector surface emitting laser with periodic gain," *IEEE Photon. Technol. Lett.*, vol. **1**, no. 3, pp. 52–54 (1989).

39 R. S. Geels, and L. A. Coldren: "Sub-milliamp threshold vertical-cavity laser diodes," *Appl. Phys. Lett.*, Vol. **57**, pp. 1605–1607, (1991)

40 R. A. Morgan, "High-performance, producible vertical-cavity lasers for optical interconnect," in *Current Trends in Vertical Cavity Surface Emitting Lasers*, T. P. Lee Ed., World Scientific, pp. 65–95 (1995).

41 T. Wipiejewski, K. Panzlaf, E. Zeeb, and K. J. Ebeling, "Sub-milliamp vertical cavity laser diode structure with 2.2 nm continuous tuning," 18th European Conf. Opt. Comm. '1992, PD II-4, Sept. 1992.

42 Y. Hayashi, T. Mukaihara, N. Hatori, Ohnoki, A. Matsutani, F. Koyama, and K. Iga, "Record low-threshold index-guided InGaAs/GaAlAs vertical-cavity surface-emitting laser with a native oxide confinement structure," *Electron. Lett.*, vol. **31**, no. 7, pp. 560–561, Mar. (1995).

43 J. M. Dallesasse, N. Holonyak Jr., A. R. Sugg, T. A. Richard, and N. El-Zein: "Hydrolyzation-oxidation of $Al_xGa_{1-x}As$-AlAs-GaAs quantum well heterostructures and superlattices," *Appl. Phys. Lett.*, vol. **57**, no. 26, pp. 2844–2846 (1990).

44 M. H. Crawford, K. D. Choquette, R. J. Hickman, and K. M. Geib, "Performances of selective oxidized AlGaInP-based visible VCSELs," in *OSA Trends in Optics and Photonics (Advances in Vertical Cavity Surface Emitting Laser)*, Ed. C. Chang-Hasnain, vol. **TOPS15**, pp. 112–117 (1997).

45 N. Yokouchi, T. Miyamoto, T Uchida, Y Inaba, F. Koyama, and K. Iga, "40 Å continuous tuning of a GaInAsP/InP vertical-cavity surface-emitting laser using an external mirror," *IEEE Photon. Technol. Lett.*, vol. **4**, no. 7, pp. 701–703, July (1992).

46 M. S. Wu, E. C. Vail, G. S. Li, W. Yuen, and C. J. Chang-Hasnain, "Tunable micromachined vertical cavity surface emitting laser," *Electron. Lett.*, vol. **31**, no. 19, pp. 1671–1672 (1995).

47 E. Ho, F. Koyama, and K. Iga: "Effective reflectivity from self-imaging in a Talbot cavity and its effect on the threshold of a finite 2-D surface emitting laser array," *Appl. Opt.*, vol. **29**, no. 34, pp. 5080–5085 (1990).

48 T. Baba, Y. Yogo, K. Suzuki, F. Koyama, and K. Iga, "Near room temperature continuous wave lasing characteristics of GalnAsP/lnP surface emitting laser," *Electron. Lett.*, vol. **29**, no. 10, pp. 913–914 (1993).

49 K. Iga, "Surface emitting laser-its birth and generation of new optoelectronic fields," *IEEE J. Sel. Top. Quantum Electron.*, Invited paper, vol. **6**, No. 6, pp. 1201–1215, Nov./Dec., 2000.

50 E. Towe, R. F. Leheny, and A. Yang, (December 2000). "A historical perspective of the development of the vertical-cavity surface-emitting laser". *IEEE J. Sel. Top. Quantum Electron*., vol. **6**, no. 6, pp. 1458–1464, Nov./Dec., 2000.

51 C. J. Chang-Hasnain, J. P. Harbison, C. E. Zah, M. W. Maeda, L. T. Florez, N. G. Stoffel, and T. P. Lee: "Multiple wavelength tunable surface-emitting laser arrays,," *IEEE J. Quantum Electron.*, vol. **27**, no. 6, pp. 1368–1376 (1991).

52 B. D. Padullaparthi, R. Chen and A. Tan et al., "High Volume Manufacturing of VCSELs for Datacom & Sensing," Industry Panel Discussions, Th4, pp: 51, International Nano-Optoelectronics Workshop (i-NOW) 2018, UC Berkeley, USA.

53 K. Iga, F. Koyama, and S. Kinoshita, "Surface emitting semiconductor laser," *IEEE J. Quantum. Electron.*, vol. **QE-24**, no. 9, pp. 1845–1855, Sept. (1988).

54 C. Jung, R. Jäger, M. Grabherr, P. Schnitzer, R. Michalzik, B. Weigl, S. Muller, and K. J. Ebeling, "4.8 mW single mode oxide confined top-surface emitting vertical-cavity laser diodes," *Electron. Lett.*, vol. **33**, no. 21, pp. 1790–1791 (1997).

55 K. Iga, "Forty years of VCSEL: Invention and innovation," *Jpn. J. Appl. Phys.* Vol. **57**, No. 8S2, pp. 1–7, Aug. (2018).

56 B. D. Padullaparthi, "Impact of Δn_{eff} of 850nm VCSEL cavity on low noise for 100G eSR4 transmission and its potential for ≥400G datacenter optical interconnects," *Proc. SPIE* **11704** 11704–24 (2021) doi:10.1117/12.475724.

57 J. A. Tatum and J. K. Guenter, "The VCSELS are coming," Proc. SPIE 4994, Vertical-Cavity Surface-Emitting Lasers VII, 17 June 2003;

58 K. Iga, "VCSEL Odyssey," SPIE No. PM318, September 1, 2020.